IEEE Access
Multidisciplinary | Rapid Review | Open Access Journal

Received March 22, 2021, accepted March 30, 2021, date of publication April 9, 2021, date of current version April 20, 2021.

Digital Object Identifier 10.1109/ACCESS.2021.3072104

Optimization Method of Dynamic Beam Position for LEO Beam-Hopping Satellite Communication Systems

JINGYU TANG, DONGMING BIAN, GUANGXIA LI, JING HU, AND JIAN CHENG
College of Communications Engineering, Army Engineering University of PLA, Nanjing 210007, China
Corresponding author: Dongming Bian (biandm_satlab@163.com)

ABSTRACT The beam-hopping (BH) technology applied to low earth orbit (LEO) satellite communication networks is a superior choice, but the long transmission delay partly caused by data packets waiting in the queue of satellite transponders will seriously affect the user experience. To shorten the packet queueing delay, in this paper, we propose an optimization method of dynamic beam position division for LEO BH satellite communication systems. Firstly, we analyze the packet queueing delay problem in BH satellites to find out the factors related to the queueing delay, and we find that the number of beam positions is negatively correlated with the queueing delay. Then, we turn the beam position division problem into a *p*-center problem to try to cover all users with the least number of beam positions. The beam positions among the footprint of LEO satellites are determined dynamically by the user distribution and the traffic distribution. Finally, the performance evaluation of the proposed optimization method is carried out in real-time and the simulation shows that the beam position division optimized system we proposed can shorten the queueing delay up to 40% compare to the benchmark system without sacrificing throughput.

INDEX TERMS LEO satellite communication system, beam-hopping, beam position optimization, packet queueing delay, *p*-center problem.

I. INTRODUCTION

LEO satellite communication networks can provide full-time communication services without blind zones, which is an incomparable advantage over ground communication networks. With the increasing demand for Internet access, LEO satellite communication networks will play a more important role in the fifth-generation (5G) and the upcoming sixth-generation (6G) mobile communication networks. Nowadays, a new round boom of the LEO satellite constellation system has risen and become a hotspot of commercial investment, including OneWeb [1], SpaceX [1], Telesat [2], and other satellite-related companies that have put forward their commercial LEO satellite constellation systems.

After the retreat of the LEO satellite constellation system upsurge represented by the Iridium system in the 1990s, one of the keys to the success of this round boom lies in cost control. Satellite miniaturization which can reduce the cost of satellite manufacturing, launching, and maintaining is a cost-effective way since thousands of satellites are needed for an LEO satellite constellation system. However, small satellites mean limited payload capacity, and how to ensure the service quality of small satellites is a primary consideration. The beam-hopping (BH) technology seems to be a candidate technology to solve the conflict between satellite miniaturization and payload capacity limitation. Compared with the conventional multibeam satellite, the BH satellite applied in LEO satellite communication networks has its unique advantages, mainly in the following aspects:

- The BH satellite shares antennas and transmitters among all beams, which is helpful for the miniaturization of satellites.
- The BH satellite has high effective isotropic radiated power (EIRP) and G/T value (receiving antenna gain divided by equivalent noise temperature), which is helpful for the miniaturization of the user terminals.
- The traffic distribution in the footprint of the satellite is non-uniform. BH satellites can allocate resources in four dimensions including space, time, bandwidth, and power. Compared with multibeam satellites, BH satellites have higher flexibility in resource allocation.

The associate editor coordinating the review of this manuscript and approving it for publication was Hayder Al-Hraishawi.

- The BH satellite has higher energy efficiency compared with multibeam satellites.

However, one of the disadvantages of the BH satellite is its high latency. Data packets for downlink transmission need to wait in the queue of the satellite transponder until the corresponding spot-beam is illuminated. The BH technology applied to high throughput satellites usually adopts a regular time window which ranges from tens to hundreds of milliseconds to allocate spot-beams periodically [3]. Obviously, the average packet queueing delay approximately equal to half the time window which accounts for a large part of the whole transmission delay. The long time delay will seriously reduce the quality of experience (QoE) especially for real-time communication and multimedia services. To shorten the queueing delay, in this paper, we analyze the downlink capacity and packet queuing delay of LEO BH satellite systems, and the corresponding theoretical expressions are given. According to the theoretical expressions, the delay-related factors are discussed to find a way to shorten the packet queueing delay. We propose an optimization method of dynamic beam position division for LEO BH satellite systems. Distinguish from static or passive beam position division, the proposed optimization method can dynamically search the beam positions among the footprint of the LEO satellite by the user distribution and the traffic demand distribution. The simulation results show that our optimization method can effectively shorten the packet queueing delay in the satellite transponder with the traffic demand is guaranteed and without sacrificing throughput.

The rest of this paper is organized as follows: Section II introduces the related works about BH technology applied to satellite systems. Section III describes the LEO BH satellite system model and analyzes the packet queueing delay problem in BH satellite systems. Section IV introduces the *p*-center problem algorithm used in our optimization method. In Section V, we present the beam position division optimization method. Section VI presents and analyzes the simulation results. Section VII concludes this paper.

II. RELATED WORK

The BH technology is developed from multibeam technology and has been successfully applied to the Spaceway3 system [4] and the Eutelsat Quantum satellite [5]. The performance comparison between BH satellites and multibeam satellites has been widely studied. Mokhtar *et al.* analyzed the downlink throughput of a broadband LEO satellite network with BH, and the upper and lower bounds on the downlink throughput were given [6]. In [7], Angeletti *et al.* focused on the application scenario of multibeam satellite systems to provide broadband multimedia access for users in sparsely distributed areas and analyzed the effect of BH technology on improving the performance of the whole system. A throughput increase of about 30% compared to a system with regular power and bandwidth allocation capabilities was achieved. In [8] and [9], the system simulation and performance comparison between BH systems and non-hopped systems were evaluated based on the predicted traffic demands for 2010 from the original ESA DDSO (Digital Divide Satellite Offer) study [10]. In [11], the BH transmission scheme, focusing on the forward link, was investigated. Simulation results have shown that BH satellite systems outperform the conventional system in terms of both adaptation throughput matching traffic demands and more efficient use of available resources. In [12], the BH transmission scheme was compared with the non-orthogonal frequency reuse (NOFR) transmission scheme, and the study of the resource optimization have shown that the BH system performs slightly better than NOFR.

The resource allocation optimization of BH satellite systems is another research hotspot. In [13]–[17], researchers optimized beam allocation to improve the system throughput or matched traffic demands with allocated capacities. In [18] and [19], optimum power allocation in BH systems was studied. In [20], a beam resource management algorithm that adjusts the beam size according to the traffic distribution was proposed, which can let more users access the satellite and make full use of beam bandwidth resources by covering more beam positions. In [21], Han *et al.* focused on the delay fairness of each cell in the BH system, and a delay fairness-oriented BH algorithm was proposed. In [22]–[24], BH was combined with deep learning or deep reinforcement learning, which provides a novel optimization method to obtain the BH transmission scheme.

Besides, BH technology was also used in cognitive satellite systems based on the spatial isolation of spot-beam to improve the throughput and spectrum efficiency of systems [25].

The literature review reveals that there is little research that focuses on the delay problem on BH satellite systems. The reference [21] pays attention to the delay fairness for BH satellite systems, but it didn't try to shorten the transmission delay. However, the transmission delay is a very important indicator for most users, which may determine whether users use the system or not. Thus, the delay problem is worthy of further study to let users get better QoE.

III. SYSTEM MODEL AND ANALYSIS

A. SYSTEM MODEL

This paper considers a Walker constellation of the LEO satellite communication system operating at Ka-band. The earth surface is divided into hundreds of satellite coverage areas and each coverage area is served by a BH satellite, as shown in Fig. 1. The BH satellites will move at high speed relative to the ground but the locations of the coverage areas are fixed. Each satellite is equipped with a phased array antenna that can focus the spot-beam on a subarea which is also called a cell in this paper within a period of time. In order to avoid confusion, in the rest of this paper, cell and beam position have the same meaning. Fig. 2 shows the diagram of the phased array antenna that the antenna can form a limited number of spot-beams and change the direction of spot-beams

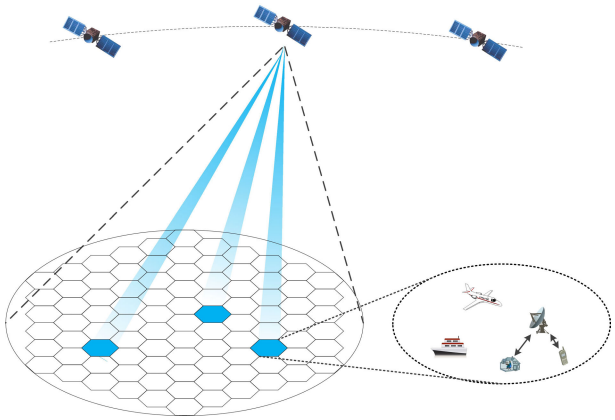

FIGURE 1. The application scenarios of LEO BH satellite systems.

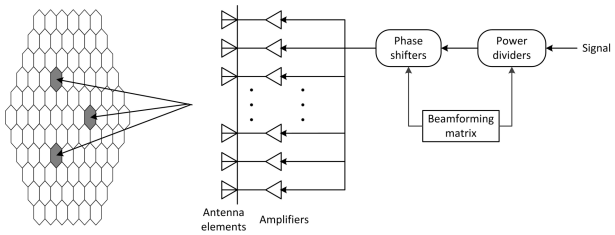

FIGURE 2. The diagram of phased array antennas.

in real-time. In the application scenario, as a supplement to the ground communication network, the LEO satellite communication system mainly serves low telecommunications infrastructure areas and mobile hotspot terminals (HTs) such as aircraft, ocean fishing boats, highspeed rails, outdoor vehicles, etc. HTs are equipped with satellite signal transceivers, which also have Wi-Fi functions. BH satellites are facing directly to HTs to implement high-speed wireless communication at Ka-band. Common user terminals realize network access through Wi-Fi.

We focus on the downlink which is based on BH technology, and the packet queueing delay problem in the satellite transponder is what we are interested in. The application scenario determines that the HTs in most of the coverage areas are scarce. Fig. 3 shows the HT distribution in a coverage area, and the cell distribution under a traditional multibeam satellite. In the multibeam coverage mode, there are no HTs in some cells, and some HTs that could be covered by one cell are distributed in different cells. Therefore, the satellite resources will be waste inevitably with traditional multibeam satellites when the HTs are scarce.

B. THE ANALYSIS OF LEO BH SATELLITE SYSTEMS

The mechanism of BH communication makes HTs not continuously connect with satellites, therefore, the packets in the satellite transponder can't be sent to HTs in time. We analyzed the packet queueing delay problem in BH satellite transponders to find out the factors that affect the queuing delay. We assume that N_T HTs are located in the coverage area,

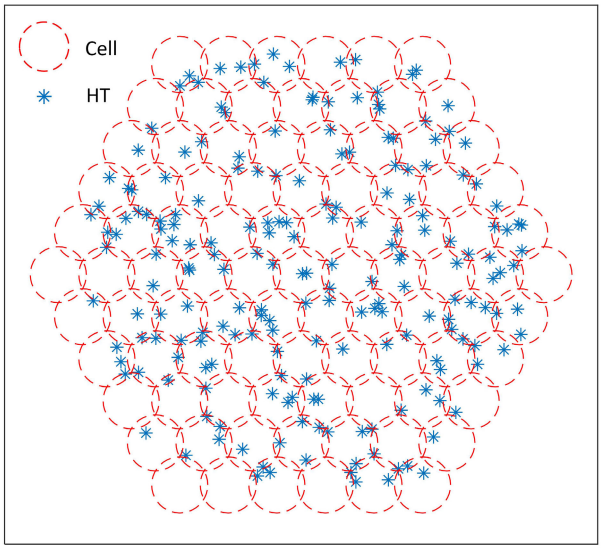

FIGURE 3. The HT distribution and the cell distribution in a coverage area.

and the average packet arrival rate (data packets arrived in the satellite transponder) for the ith HT is denoted as A_i. The packets have the same length L_p without loss of generality. All the HTs are covered by N_c cells so that the average packet arrival rate for the jth cell is given by:

$$A_j^c = \sum_{i \in U_j} A_i, \tag{1}$$

where U_j denotes the set of HTs that belong to the jth cell, $U_i \cap U_j = \varnothing$ for $\forall i \neq j$. The communication capacity based on Shannon's capacity for the jth cell is given by:

$$C_j = B_{tot} \log_2 \left(1 + \frac{\alpha_j P_{tot}}{N_b n_0 B_{tot}}\right), \tag{2}$$

where B_{tot} and P_{tot} denotes the total bandwidth and power respectively for the downlink, α_j denotes the channel coefficient from the satellite to the jth cell, N_b denotes the limited (or maximum) number of spot-beams, and n_0 denotes the power spectral density of noise. Each spot-beam is allowed to use the total bandwidth and the total power is uniformly allocated to N_b spot-beams. It is assumed that the HTs should regularly report some necessary information to the beam-hoping satellite, and the channel state is included in this information. The channel state can be obtained either through direct channel measurement or through a combination of measurement and channel prediction.

The BH pattern is vital for the stability of the BH satellite system. The stability here mainly refers to the limited packet queue for every cell that will not be jammed. Let x_i denotes the time that the ith cell is illuminated during the time interval $[0, T]$ in a steady state. Then, for each packet queue, the entire incoming traffic during the time interval $[0, T]$ for the ith cell should be less than the total capacity allocated, that is:

$$A_i^c L_p \cdot T \leqslant x_i \cdot C_i \Rightarrow \frac{A_i^c L_p}{C_i} \leqslant \frac{x_i}{T}. \tag{3}$$

Since $x_i \leqslant T$, and substituting (2) into (3), we obtain:

$$\frac{A_i^c L_p}{B_{tot} \log_2\left(1+\frac{\alpha_i P_{tot}}{N_b n_0 B_{tot}}\right)} \leqslant 1. \tag{4}$$

For the whole system, we ignore the influence of co-channel interference (CCI) between beams for the time being, and sum both sides of (3) over i, we obtain:

$$\sum_{i=1}^{N_c} \frac{A_i^c L_p}{C_i} = \sum_{i=1}^{N_c} \frac{A_i^c L_p}{B_{tot} \log_2\left(1+\frac{\alpha_i P_{tot}}{N_b n_0 B_{tot}}\right)} \leqslant \sum_{i=1}^{N_c} \frac{x_i}{T} \leqslant N_b. \tag{5}$$

Similar results are also shown in [19] and [26]. Since the function $\log_2(1+k/x)$ is monotonically decreasing and the function $x\log_2(1+k/x)$ is monotonically increasing concerning x for $\forall k > 0$, if feasible, an appropriate number N_b should be selected to satisfy the constraint (4) and (5) simultaneously.

For downlink transmission, intuitively, the policy of selecting the N_b largest queues (abbreviated as Largest Queues Policy, LQP) or the N_b fastest nonempty queues (abbreviated as Fastest Queues Policy, FQP) to transmit in each transmission cycle would maximize throughput and achieve stability. But [19] has proved that the FQP is more unstable than the LQP, and an example is given. Consider a three-cell two-beam system with constant communication capacities $(C_1, C_2, C_3) = (2, 2, 1)$ and constant packet arrival rates $\left(A_1^c, A_2^c, A_3^c\right) = (1, 1, 1/2)$. All arriving packets have the same length $L_p = 1$. According to the FQP, the two beams will always serve cells 1 and 2 which makes cell 3 jammed. However, the system is clearly stable by the LQP. To get a stable system, the LQP is what we base on when designing the BH pattern, and basing on this policy we have further analysis of the communication capacity and the queueing delay of the BH satellite.

The throughput of a BH satellite is time-variant with the different cells are illuminated, but in the long term, the average percentage of time $\left(T_{p1}, T_{p2}, \ldots, T_{pN_c}\right)$ that each cell is illuminated should be:

$$T_{p1} : T_{p2} : \ldots : T_{pN_c} = \frac{A_1^c L_p}{C_1} : \frac{A_2^c L_p}{C_2} : \cdots : \frac{A_{N_c}^c L_p}{C_{N_c}}. \tag{6}$$

That is to say, the LQP is proportionally fair for each cell. In this paper, we define the communication capacity C_S of the BH satellite as:

$$C_S\left(A_1^c, A_2^c, \ldots, A_{N_c}^c; N_b\right) = N_b \cdot \sum_{i=1}^{N_c} \frac{\frac{A_i^c L_p}{C_i}}{\sum_{j=1}^{N_c} \frac{A_j^c L_p}{C_j}} \cdot C_i = \frac{N_b \sum_{j=1}^{N_c} A_i^c}{\sum_{j=1}^{N_c} \frac{A_j^c}{C_j}}. \tag{7}$$

It is noteworthy that the $A_1^c, A_2^c, \ldots, A_{N_c}^c$ in (7) doesn't mean that when the ith cell's average packet arrival rate must be equal to A_i^c that the BH satellite has the communication capacity $C_S\left(A_1^c, A_2^c, \ldots, A_{N_c}^c; N_b\right)$. In fact, $C_S\left(\rho A_1^c, \rho A_2^c, \ldots, \rho A_{N_c}^c; N_b\right) = C_S\left(A_1^c, A_2^c, \ldots, A_{N_c}^c; N_b\right)$ for any positive value ρ.

Concerning the queueing delay, let $Z(T)$ denotes the summed packet number arriving into the satellite transponder during the period $[0, T]$, and $N(t)$ denotes the packet number in time instant t in the satellite transponder. According to the queuing theory, the total queueing time overall the packets is the integral of the instantaneous packet number multiplied by time [21]. So the average queueing delay Q could be transformed into:

$$Q = \lim_{T\to\infty} \frac{1}{Z(T)} \int_0^T N(t)dt. \tag{8}$$

Taking expectation on both sides of (8), we obtain:

$$\begin{aligned} &E[Q] \\ &= \lim_{T\to\infty} \frac{1}{E[Z(T)]} \int_0^T E[N(t)]dt \\ &= \lim_{T\to\infty} \frac{1}{T\sum_{i=1}^{N_c} A_i^c L_p} \int_0^T \sum_{i=1}^{N_c} E[N_i(t)]dt \\ &= \lim_{n\to\infty} \frac{1}{n\Delta t \sum_{i=1}^{N_c} A_i^c L_p} \sum_{m=1}^{n} \int_{(m-1)\Delta t}^{m\Delta t} \sum_{i=1}^{N_c} E[N_i(t)]dt, \end{aligned} \tag{9}$$

where $N_i(t)$ denotes the packet number in time instant t in the satellite transponder and should be transmitted to the ith cell, and Δt is a timeslot which is the minimum time unit. Our system switch beams every timeslot[1] based on the LQP, so the timeslot Δt can't be too long or too short. Too long a timeslot causes a long queueing delay, and too short a timeslot is not time-abundant to let the system be prepared for transmission in the next timeslot. Now let us consider the change from $N_i(m\Delta t)$ to $N_i(m\Delta t + \Delta t)$, in (10), as shown at the bottom of the page. ΔA_m denotes the number of arriving packets during $(m\Delta t, m\Delta t + \Delta t)$, and when the ith cell is illuminated in this period, $\Phi_i(m) = 1$, otherwise, $\Phi_i(m) = 0$.

The change of the number of packets in a timeslot illustrates that the packets arrived during the illumination timeslot

[1]This is different from BH systems with BH time window. Those systems usually allocate continuous timeslots to cells within the BH time window, which causes longer queueing delay than our system.

$$N_i(m\Delta t + \Delta t) - N_i(m\Delta t) = \begin{cases} N_i(m\Delta t) + \Delta A_m, & \Phi_i(m) = 0 \\ N_i(m\Delta t) - C_i\Delta t/L_p + \Delta A_m, & \Phi_i(m) = 1 \text{ and } N_i(m\Delta t) > C_i\Delta t/L_p \\ \Delta A_m, & \Phi_i(m) = 1 \text{ and } N_i(m\Delta t) \leqslant C_i\Delta t/L_p \end{cases} \tag{10}$$

will not be transmitted immediately in this timeslot, and we can reasonably deduce that the average illumination interval T_{qi} between two consecutive illumination timeslot for the ith cell is negatively correlated with the average percentage of illumination time T_{pi}, that is:

$$T_{q1} : T_{q2} : \cdots : T_{qN_c} = \frac{C_1}{A_1^c L_p} : \frac{C_2}{A_2^c L_p} : \cdots : \frac{C_{N_c}}{A_{N_c}^c L_p}. \quad (11)$$

For the ith cell, there is:

$$\Delta t : T_{qi} = N_b \cdot \frac{A_i^c L_p}{C_i} : \sum_{j=1}^{N_c} \frac{A_j^c L_p}{C_j}. \quad (12)$$

We have:

$$T_{qi} = \frac{\Delta t}{N_b} \cdot \frac{\sum_{j=1}^{N_c} \frac{A_j^c}{C_j}}{\frac{A_i^c}{C_i}}. \quad (13)$$

Since the packets arrive evenly on the time axis, the average queueing delay $Q_S\left(A_1^c, A_2^c, \ldots, A_{N_c}^c; N_b; \Delta t\right)$ for the whole system is:

$$Q_S\left(A_1^c, A_2^c, \ldots, A_{N_c}^c; N_b; \Delta t\right) = \sum_{i=1}^{N_c} \frac{\frac{T_{qi}}{2} A_i^c}{\sum_{j=1}^{N_c} A_j^c}. \quad (14)$$

Substituting (13) into (14), we obtain:

$$Q_S\left(A_1^c, A_2^c, \ldots, A_{N_c}^c; N_b; \Delta t\right) = \frac{\Delta t}{2N_b} \cdot \frac{\sum_{i=1}^{N_c} C_i \sum_{k=1}^{N_c} \frac{A_k^c}{C_k}}{\sum_{j=1}^{N_c} A_j^c}. \quad (15)$$

After the previous analysis, (7) and (15) show the communication capacity and the average queueing delay respectively for the BH system with the LQP. Our purpose is to shorten the average queuing delay as much as possible in the case of satisfying the traffic demand. The related parameters including Δt, N_b, and N_c, while the value of Δt and the number of N_b are pre-defined in the system design according to the hardware conditions. The number of N_c is optimizable benefiting from the beam of phased array antenna can be pointed arbitrarily. Hence, the optimized cell division with a minimal number of cells will shorten the average queuing delay effectively, which we will introduce in the next section.

C. CCI CONSTRAINTS

When analyzing the stability of the system, we ignore the influence of CCI between beams for the time being. In fact, as is shown in Fig. 2(b), some adjacent cells are close enough that there will be CCI when those cells are illuminated at the same time. Hence, an interference avoidance mechanism is needed. According to the radiation pattern of the phased array antenna, when the distance between two beams is large enough, the CCI between beams will be so weak that it can be ignored. Based on this characteristic, we set a *keep-out radius* R_k for all cells as the minimum spatial isolation distance between any two cells. We consider an interference matrix $M = \left[\Upsilon_{ij}\right]_{N_c \times N_c}$, and we have:

$$\Upsilon_{ij} = \begin{cases} 1, & D_{ij} < R_k \\ 0, & D_{ij} \geqslant R_k. \end{cases} \quad (16)$$

where D_{ij} denotes the distance between the centers of the cell i and the cell j, $\Upsilon_{ij} = 1$ represents that there is CCI between cell i and cell j, otherwise $\Upsilon_{ij} = 0$. The cell set is represented as $\mathcal{C} = \left\{\mathfrak{c}_1, \mathfrak{c}_2, \ldots, \mathfrak{c}_{N_c}\right\}$, and we define an *interference group* $\mathcal{I} = \left\{I_1, I_2, \ldots, I_{N_I}\right\}$ which can be extracted from the interference matrix M. Interference group $\mathcal{I}$ and set I_k are defined with the following properties:

Property 1: $D_{ij} < R_k$ for $\forall \mathfrak{c}_i, \mathfrak{c}_j \in I_k$.
Property 2: $I_i \not\subset I_j$ for $\forall I_i, I_j \in \mathcal{I}$.
Property 3: $\forall \mathfrak{c}_l \notin I_k$ and $l \in \mathcal{C}$, $\exists \mathfrak{c}_j \in I_k$ let $D_{lj} \geqslant R_k$.
Property 4: $\forall \mathfrak{c}_i, \mathfrak{c}_j \in \mathcal{C}$ and $D_{ij} < R_k$, $\exists I_k \in \mathcal{I}$ let $\left\{\mathfrak{c}_i, \mathfrak{c}_j\right\} \subseteq I_k$.

Each set I_k in the interference group $\mathcal{I}$ means that any two cells in the set I_k can't be simultaneously illuminated based on the interference avoidance mechanism. To achieve stability over the cells in any set $I_k \in \mathcal{I}$, refer to (5), we obtain:

$$\sum_{i \in I_k} \frac{A_i^c L_p}{C_i} \leqslant 1 \quad for\ \forall k = 1, 2, \ldots, N_I. \quad (17)$$

Inequalities (4), (5) and (17) give the constraints for the stability of the system. The local area with overload traffic may need a congestion control strategy to satisfy all the constraints. It should be clarified that the constraint (17) is not unique to BH systems, and multibeam systems will also face a similar constraint.

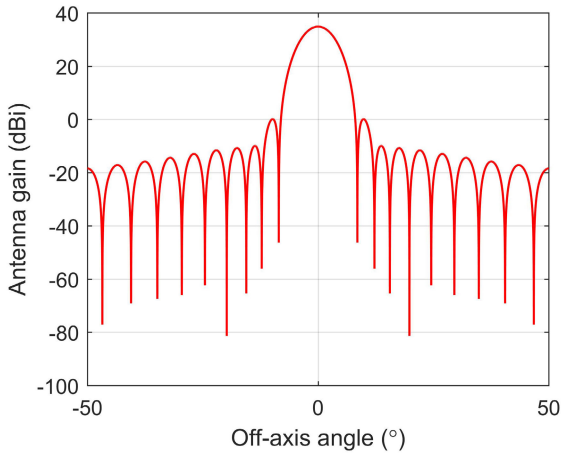

FIGURE 4. The diagram of phased array antennas.

IV. P-CENTER PROBLEM ALGORITHM

Covering all the HTs with a minimal number of cells is an effective way to shorten the average queueing delay. In our systems, the hopping beam is the circular beam, as is shown in Fig. 4, and its radiation pattern (simplified) [27]

is given by:

$$G_t(\theta) = G_0\left[\frac{J_1(u(\theta))}{2u(\theta)} + 36\frac{J_3(u(\theta))}{u(\theta)^3}\right], \tag{18}$$

where θ is the off-axis angle, G_0 is the peak beam gain defined as $G_0 = \eta N^2\pi^2/\theta_{3dB}^2$, η is the antenna efficiency generally equal to 0.65, $N = 65$ for phased array antenna, θ_{3dB} is the 3dB gain angle of the antenna, $J_1(\cdot)$ and $J_3(\cdot)$ represent the Bessel function of the first kind and the third kind respectively, $u(\theta) = 2.07123\sin\theta/\sin\theta_{3dB}$.

The problem that covering all the HTs with the minimal number of cells is a derivative problem of p-center problem [28], [29] in plane geometry for the circular cells. p-center problem can be defined as follows: given a set $S = \{s_1, s_2, \ldots, s_n\}$ of n points in a plane, p-center problem seeks the location of p centers $c_1, c_2, \ldots, c_p$ such that the maximum distance of any given point from its closest center is minimized, that is:

$$\min_{c_1,c_2,\ldots,c_p}\left\{\max_{1\leqslant i\leqslant n}\left\{\min_{1\leqslant j\leqslant p} d\left(s_i, c_j\right)\right\}\right\}, \tag{19}$$

where $d(a, b)$ is the Euclidean distance between two points a and b which are located at $a(x_a, y_a)$ and $b(x_b, y_b)$ respectively. It is assumed that the set of all the HTs in a coverage area is $\mathcal{U} = \{u_1, u_2, \ldots, u_{N_T}\}$ and the maximum cell radius is $r_{\max}$. The problem of finding the minimal number of cells is translated to the problem of finding the smallest integer p that satisfied the constraint:

$$r_{\max} \geqslant \min_{c_1,c_2,\ldots,c_p}\left\{\max_{1\leqslant i\leqslant N}\left\{\min_{1\leqslant j\leqslant p} d\left(u_i, c_j\right)\right\}\right\}. \tag{20}$$

Basing on the p-center algorithm in [29], we make a little modification in our p-center algorithm.

Let us define some concepts that we shall need later. Let $F(\Lambda)$ be the minimum distance for the 1-center problem consisting of the points of Λ. $F(\Lambda)$ is given by:

$$F(\Lambda) = \min_{X^*}\left\{\max_{s_i\in\Lambda}\left\{d\left(s_i, X^*\right)\right\}\right\}, \tag{21}$$

and $X^*(\Lambda)$ is the optimal center of the problem (21). The following lemma is self-evident.

Lemma 1: If $\Lambda \subset \Omega$, then $F(\Lambda) \leqslant F(\Omega)$.

For the 1-center problem based on all points of the set Λ, there exists a subset $B(\Lambda)$ of no more than three points with the following properties:

Property 1: $F(B(\Lambda)) = F(\Lambda)$.

Property 2: $X^*(B(\Lambda)) = X^*(\Lambda)$.

$B(\Lambda)$ is called the "binding subset".

Lemma 2: If $s_i \in \Lambda$ and $s_i \notin B(\Lambda)$, then $F(\Lambda - \{s_i\}) = F(\Lambda)$.

Proof: Since $B(\Lambda) \subseteq \Lambda - \{s_i\} \subseteq \Lambda$, by Lemma 1, $F(B(\Lambda)) \leqslant F(\Lambda - \{s_i\}) \leqslant F(\Lambda)$. By property 1, $F(B(\Lambda)) = F(\Lambda)$. Hence, $F(\Lambda - \{s_i\}) = F(\Lambda)$.

We take a case of 8 points $\{s_1, \ldots, s_8\}$ and 3 centers $\{c_1, c_2, c_3\}$ for example, as shown in Fig. 5.

Step 1: Randomly select three points as centers out of the point set, as shown in Fig. 5(a), and each point is assigned to the center which is the nearest to the point. If a point can belong to more than one center, assign it arbitrarily to one center. The point set is divided into 3 subsets $\{\Lambda_1, \Lambda_2, \Lambda_3\}$ that $\Lambda_i = \left\{s_k | d\left(s_k, c_i\right) \leqslant d\left(s_k, c_j\right), \forall i \neq j\right\}$.

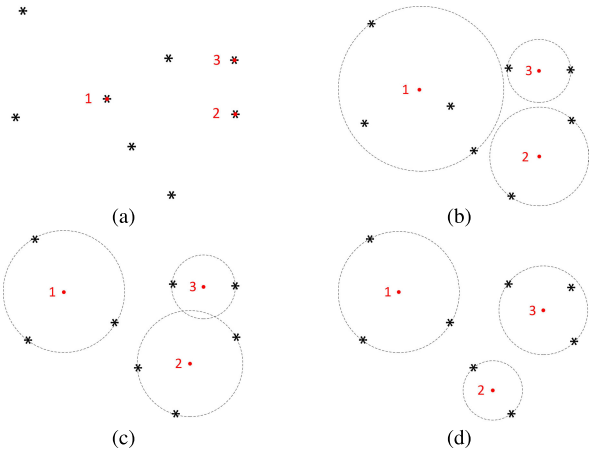

FIGURE 5. An example of the *p*-center algorithm.

Step 2: Update the centers for the 3 subsets, as shown from Fig. 5(a) to Fig. 5(b).

Step 3: Consider a rearrangement at a time that removes point s_i from Λ_j and add it to another subset Λ_k if $\max\{F(\Lambda_j - \{s_i\}), F(\Lambda_k + \{s_i\})\} < \max\{F(\Lambda_j), F(\Lambda_k)\}$, as shown from Fig. 5(b) to Fig. 5(c). By Lemma 1, only the value of $F(\Lambda_j)$ may decrease. By Lemma 2, the value of $F(\Lambda_j)$ may decrease by the rearrangement only if $s_i \in B(\Lambda_j)$. So we should select the point out of the binding subset of Λ_j and add it to the subset Λ_k that $F(\Lambda_j) > F(\Lambda_k)$.

Step 2 and step 3 are applied alternately until neither changes the partition. The p-center algorithm in [29] only searches the minimum distance from points to centers, and in our example, it will stop at the state shown in Fig. 5(c). However, the division of subset 2 and subset 3 can still be optimized such as from Fig. 5(c) to Fig. 5(d). This is the difference between our p-center algorithm and the p-center algorithm in [29]. It is quite important to separate adjacent cells and shrink the cell radius as much as possible, the former is for less CCI between adjacent cells and the latter is for higher received power.

V. CELL DIVISION OPTIMIZATION

A. CELLS SELECTION

Due to the interference avoidance mechanism, the LQP should be modified a little without affecting the results of the previous analysis. The cell selection algorithm is shown in Algorithm 1. The packet number at the beginning of the mth timeslot in the ith queue is denoted as $N_i((m-1)\Delta t)$. We select the cell from front to back based on the descending order of $N_i((m-1)\Delta t)$ for $i = 1, 2, \ldots, N_c$ at the beginning of the mth timeslot. If the selected cell will cause interference to the previously selected cells according to the interference matrix M, skip this cell and consider the next cell until N_b cells are selected.

Algorithm 1 The Cell Selection Algorithm With Interference Avoidance

Input: $N_i\left((m-1)\,\Delta t\right), N_b, M$
Output: Serial numbers of N_b selected cells C_{select}
Begin:
1: Reorder $N_i\left((m-1)\,\Delta t\right)$ in descending order obtain $\left\{N_i^1, N_j^2, \ldots, N_k^{N_c}\right\}$.
2: Set $count = 0$, $index = 1$, $C_{select} = \varnothing$.
3: **while** $count \neq N_b$ **do**
4: Select N_n^{index}.
5: **if** $\Upsilon_{nm} = 0, \forall m \in C_{select}$ **then**
6: $C_{select} = C_{select} \cup n$
7: $count = count + 1$
8: **end if**
9: $index = index + 1$
10: **end while**
End

Algorithm 2 The Cell Division Optimization Algorithm With Fixed Cell Radius

Input: The coordinates of HT $\left(x_{u_i}, y_{u_i}\right)$, r_{fix}
Output: The centers of optimized cells
Begin:
1: Set $p = 1$.
2: **while** true **do**
3: p-center problem algorithm computes $\min\limits_{c_1,c_2,\ldots,c_p}\left\{\max\limits_{1\leqslant i\leqslant N}\left\{\min\limits_{1\leqslant j\leqslant p} d\left(u_i, c_j\right)\right\}\right\}$.
4: **if** the constraint (18) is satisfied **then**
5: break
6: **else**
7: $p = p + 1$
8: **end if**
9: **end while**
10: Calculate the optimal cell center by the 1-center problem algorithm.
End

B. CELL DIVISION OPTIMIZATION

When the phased array antenna has a fixed 3dB gain angle θ_{3dB}, the cells have almost the same radius r_{fix}. The cell division optimization is a simple problem of finding the smallest integer p that satisfied the constraint (20). The cell division optimization algorithm with the fixed cell radius is summarized in Algorithm 2. In this paper, the p-center problem belongs to the absolute p-center problem. Even though we hope to find the smallest integer p, p-center problem has been proved to be an NP-hard problem. To get a better result, Algorithm 2 can be computed repeatedly to get the optimal value. According to the radiation pattern of the antenna, the HTs will receive higher signal power as they get closer to the center of the cells. Thus, we also hope that after the division of the cells to which the HTs belong, the HTs will be as close as possible to the center of the cells. In step 10 of Algorithm 2, calculating the optimal cell center is a special case of p-center problem when $p = 1$. The location of the cell center can be determined by the 1-center algorithm [30].

When the 3dB gain angle of the antenna θ_{3dB} is adjustable, and the cell radius range from r_{min} to r_{max}. It should be noted that the HTs can receive higher signal power as the θ_{3dB} is narrower. Therefore, the smaller cell has a higher transmission capacity, otherwise, the reverse. Although the smallest integer p may get with all cells' radius is r_{max}, which is what we want, it has a higher priority to satisfy the traffic demand in the coverage area. We can't increase the radius of the cells blindly, which may lead to the transmission capacity of the satellite lower than the traffic demand. The cell division optimization algorithm with the variable cell radius should satisfy the constraints (4), (5), (17) and (20). The constraint (4) indicates that the communication capacity provided to a cell should greater than the traffic demand of this cell. The constraint (5) indicates that the communication capacity provided to all cells should greater than the traffic demand of all cells. The constraint (17) indicates that the communication capacity provided to a set $I_k \in \mathcal{I}$ should greater than the total traffic demand of the cells belong to the set I_k. The constraint (20) indicates that the cell radius should not exceed the maximum allowed radius. Algorithm 3 is the cell division optimization algorithm with the variable cell radius. Similarly, the 1-center algorithm can not only locate the optimal cell center but also compute the minimal radius of each cell. Of course, the cell radius cannot be less than r_{min}.

Algorithm 3 The Cell Division Optimization Algorithm With Fixed Cell Radius

Input: The coordinates of HT $\left(x_{u_i}, y_{u_i}\right)$, r_{min} and r_{max}
Output: The centers and radii of optimized cells.
Begin:
1: Set $p = 1$.
2: **while** true **do**
3: p-center problem algorithm computes $\min\limits_{c_1,c_2,\ldots,c_p}\left\{\max\limits_{1\leqslant i\leqslant N}\left\{\min\limits_{1\leqslant j\leqslant p} d\left(u_i, c_j\right)\right\}\right\}$.
4: Compute A_i^c, C_i, M, $\mathcal{I}$
5: **if** constraints (4), (5), (17) and (20) are satisfied **then**
6: break
7: **else**
8: $p = p + 1$
9: **end if**
10: **end while**
11: Calculate the optimal cell center and minimal cell radius by the 1-center problem algorithm.
End

C. ALGORITHM COMPLEXITY ANALYSIS

We analyzed the algorithms from two aspects of space complexity and time complexity. Algorithm 1 is a simple algorithm, its space complexity is $O(1)$ and time complexity is $O(n)$. Algorithm 2 and Algorithm 3 have the same

space complexity and time complexity. The space complexity of both algorithms is $O(n)$. As for the time complexity, In [29], the lower bound of the time complexity of the p-center algorithm is $O\left(n^2\right)$. In Algorithm 2 and Algorithm 3, the p-center algorithm needs to be executed N_T times at most and the 1-center algorithm's time complexity is $O(n)$ [30]. Hence, Algorithm 2 and Algorithm 3 have the lower bound of the time complexity $O\left(n^3\right)$. Although Algorithm 2 and Algorithm 3 have cubic time complexity, our algorithm is still applicable. On the one hand, the number of HTs in satellite coverage areas is small; on the other hand, when the location of HTs does not change greatly, there is no need to optimize beam positions in real-time.

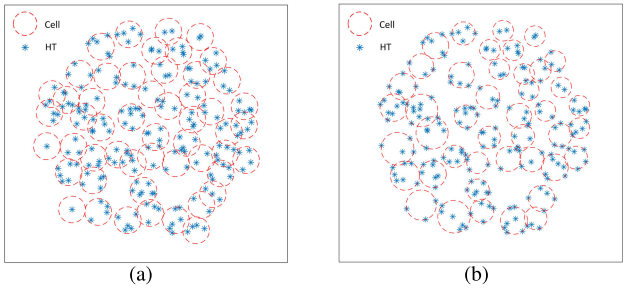

(a) (b)

FIGURE 6. The optimized cell division with fixed cell radius (a) and variable radius (b).

VI. NUMERICAL RESULTS

In this section, we simulate to verify the theoretical analysis above and show the performance of cell division optimization. As a contrast, a BH multibeam system defined in [] is presented as a benchmark system. For simplicity, the cell division optimized BH system with a variable or fixed cell radius is abbreviated as Sys 1 and Sys 2 respectively, and the BH multibeam system is abbreviated as Sys 3. The BH multibeam system fully covers a coverage area by spot-beams, but for a fair comparison, the BH multibeam system also adopts the LQP. The cell division of the BH multibeam system is shown in Fig. 3. The optimized cell division with a fixed cell radius is shown in Fig. 6(a). While the optimized cell division with variable cell radius is not only dependent on the HTs distribution but also related to the traffic distribution, and Fig. 6(b) shows one of the cell division cases. Some simulation parameters are shown in TABLE 1.

To verify the theoretical communication capacity shown in (7) and the theoretical average queueing delay shown in (15), the average packet arrival rate A_i is randomly selected in a proper range to make sure that the system reaches saturation throughput or unsaturation throughput. We compare the average throughput and the average queueing delay in the simulation time with the theoretical values of the Sys 2 and take the number of hopping beams N_b as the independent variable. The simulation results are shown in Fig. 7 and Fig. 8. The theoretical expressions show that the beam size

TABLE 1. Simulation parameters.

Parameter	Sys 1	Sys 2	Sys 3
Satellite orbit height (km)	1000	1000	1000
Total power P_{tot} (W)	100	100	100
Total bandwidth B_{tot} (MHz)	240	240	240
Maximum number of hopping beams N_b	10	10	10
Transmitting antenna peak gain G_0 (dBi)	32.3-37.1	34.8	34.8
Receiving antenna gain (dBi)	21.8	21.8	21.8
Transmitting antenna half power angle θ_{3dB} (°)	2.3-4.0	2.98	2.98
Cell radius (km)	40-70	52	52
Cell number N_c	Uncertain	52	91
Noise temperature (K)	293	293	293
Carrier frequency (GHz)	19.0	19.0	19.0
Time-slot Δt (ms)	5	5	5
Simulation time (s)	100	100	100
HTs number N_T	200	200	200
Keep-out radius R_k (km)	150	150	150

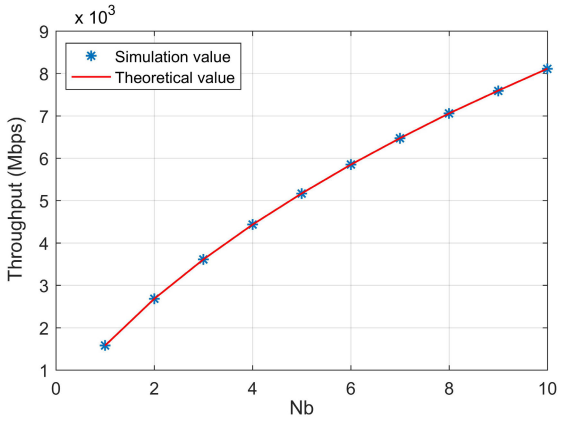

FIGURE 7. The throughput simulation of Sys 2 ($A_i \in [200, 2000]$, $L_P = 100bit$).

does not affect the communication capacity and the average queuing delay. Therefore, the simulation of Sys 2 can prove the correctness of the two theoretical expressions. The simulation values are in good agreement with the theoretical values, which means that (7) and (15) provide fairly accurate estimates for the communication capacity and the average queueing delay of the BH system with the LQP.

Fig. 9 and Fig. 10 respectively illustrate the system throughput and the queueing delay comparison among the three systems. The Sys 1 has the highest throughput and the lowest queueing delay due to its adjustable cell radius. When the traffic load is low, the Sys 1 can appropriately increase the radiation angle to cover all HTs with less

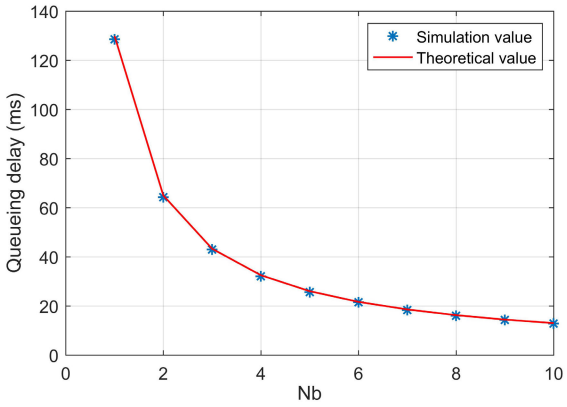

FIGURE 8. The throughput simulation of Sys 2 ($A_i \in [20, 200]$, $L_p = 100bit$).

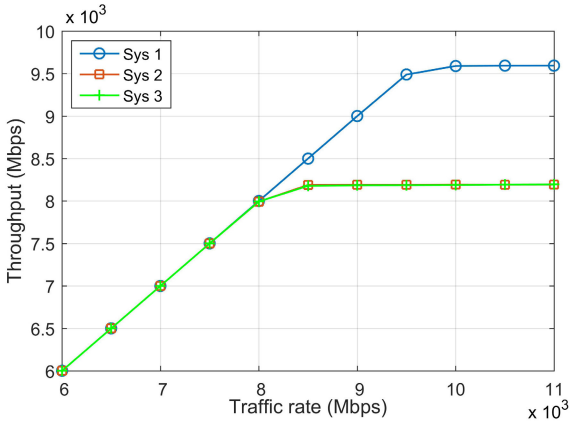

FIGURE 9. The system throughput comparison of the three systems.

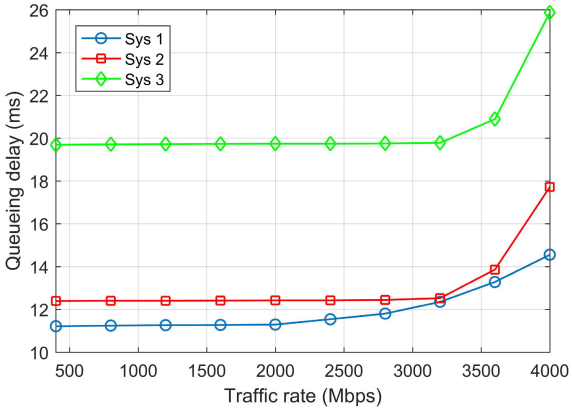

FIGURE 10. The system avarage queueing delay comparison of the three systems.

TABLE 2. Definition of possible confusing parameters and symbols.

N_T	HT number
N_b	Maximum number of hopping beams
N_c	Cell number
N_I	Element number of interference group $\mathcal{I}$
A_i	Average packet arrival rate for the ith HT
A_i^c	Average packet arrival rate for the ith cell
$\mathcal{U}$	HT set
u_i	The ith HT
U_i	Set of HTs that belong to the ith cell
$\mathcal{C}$	Cell set
$\mathfrak{c}_1$	The ith cell
C_i	Capacity of the ith cell
C_S	Capacity of the LEO satellite
c_i	Center of the ith cell
α_i	Channel coefficient from the satellite to the ith cell
T_{pi}	Average percentage of illumination time for the ith cell
T_{qi}	Average illumination interval for the ith cell
$Z(T)$	Summed packet number arriving into the satellite transponder during the period $[0, T]$
$N(t)$	Packet number in time instant t in the satellite transponder
$N_i(t)$	packet number in time instant t in the satellite transponder and should be transmitted to the ith cell
Q_S	Average queueing delay of the LEO satellite
Δt	Length of a timeslot
M	Interference matrix
$\mathcal{I}$	Interference group
I_i	An element of interference group $\mathcal{I}$
R_k	Keep-out radius
r_{fix}	Fixed cell radius
r_{min}	Minimum cell radius
r_{max}	Maximum cell radius
D_{ij}	Distance between centers of cell i and the cell j
$d(a, b)$	Distance between point a and point b
Λ, Ω	Subset of point set
$F(\Lambda)$	Minimum distance for the 1-center problem consisting of the points of Λ
$B(\Lambda)$	Binding subset of Λ

number of cells. When the traffic load is high, some cells in the Sys 2 and Sys 3 will be jammed due to the unbalanced traffic distribution, while the Sys 1 can appropriately decrease the radiation angle to obtain higher beam capacity. The Sys 2 and Sys 3 have almost the same throughput, but the queueing delay in the Sys 2 is lower than that in the Sys 3. The cell division optimized systems we proposed can shorten the queueing delay up to 40% compare to the BH multibeam system, which will greatly improve the QoE.

Fig. 10 focuses on the average queueing delay for the whole system, but it is necessary to investigate the average queueing delay for each individual HT. We simulate to show the average queueing delay of the first 100 HTs of the three systems, as shown in Fig. 11. In Sys 3, the variance of average queuing delay among HTs is larger than that in Sys 1 and Sys 2. From equation (13) we have known that the average illumination interval is traffic-related, the cell with a higher traffic load has a shorter average illumination interval, and vice versa. That is to say, the queueing delay with the LQP is not a queueing delay fairness policy for each individual HT. Some isolated HT will not get timely service. However, our cell division optimization method gathers HTs in the same cell, which reduces the number of isolated HT and makes the queueing delay fairer for each individual HT.

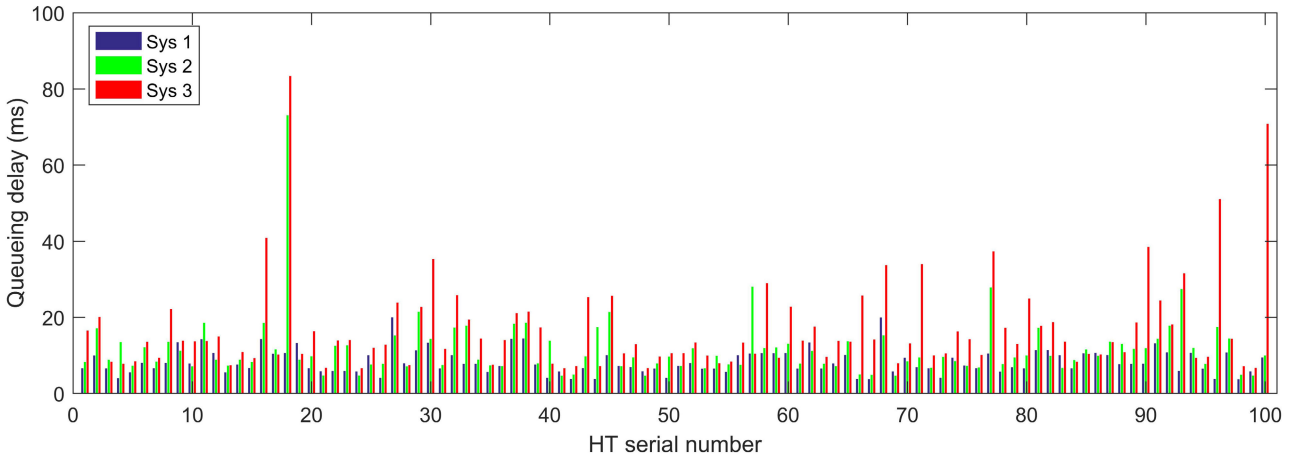

FIGURE 11. The average queueing delay for each individual HT (Traffic rate equal to 2Gbps).

VII. CONCLUSION

In this paper, a cell division optimization method for LEO BH satellite communication systems is proposed to shorten the packet queueing delay. Firstly, to achieve a stable BH satellite system, we adopt the LQP to design the BH pattern. Based on the LQP, we have further analysis of the communication capacity and the queueing delay of the BH satellite, and we find that reducing the cell number can be an effective way to shorten the packet queueing delay. Then, we turn the cell division problem into a p-center problem to try to cover all HTs with the least number of cells. The cell division optimization algorithm is proposed based on the HT distribution and the traffic distribution. Finally, the performance of the cell division optimization for the LEO BH satellite system is evaluated, and simulations show that the packet queueing delay is shortened greatly after the cell division optimization.

APPENDIX

See Table 2.

REFERENCES

[1] S. Xia, Q. Jiang, C. Zou, and G. Li, "Beam coverage comparison of LEO satellite systems based on user diversification," *IEEE Access*, vol. 7, pp. 181656–181667, 2019.

[2] I. del Portillo, B. G. Cameron, and E. F. Crawley, "A technical comparison of three low earth orbit satellite constellation systems to provide global broadband," *Acta Astronautica*, vol. 159, pp. 123–135, Jun. 2019.

[3] Y. Wang, D. Bian, J. Hu, J. Tang, and C. Wang, "A flexible resource allocation algorithm in full bandwidth beam hopping satellite systems," in *Proc. IEEE 3rd Adv. Inf. Manage., Commun., Electron. Automat. Control Conf. (IMCEC)*, Chongqing, China, Oct. 2019, pp. 920–927.

[4] R. J. F. Fang, "Broadband IP transmission over SPACEWAY satellite with on-board processing and switching," in *Proc. IEEE Global Telecommun. Conf. (GLOBECOM)*, Houston, TX, USA, Dec. 2011, pp. 1–5.

[5] H. Fenech, S. Amos, and T. Waterfield, "The role of array antennas in commercial telecommunication satellites," in *Proc. 10th Eur. Conf. Antennas Propag. (EuCAP)*, Davos, Switzerland, Apr. 2016, pp. 1–4.

[6] A. Mokhtar and M. Azizoglu, "On the downlink throughput of a broadband LEO satellite network with hopping beams," *IEEE Commun. Lett.*, vol. 4, no. 12, pp. 390–393, Dec. 2000.

[7] P. Angeletti, D. F. Prim, and R. Rinaldo, "Beam hopping in multi-beam broadband satellite systems: System performance and payload architecture analysis," in *Proc. 24th AIAA Int. Commun. Satell. Syst. Conf.*, San Diego, CA, USA, Jun. 2006, pp. 596–605.

[8] J. Anzalchi, A. Couchman, P. Gabellini, G. Gallinaro, L. D'Agristina, N. Alagha, and P. Angeletti, "Beam hopping in multi-beam broadband satellite systems: System simulation and performance comparison with non-hopped systems," in *Proc. 5th Adv. Satell. Multimedia Syst. Conf., 11th Signal Process. Space Commun. Workshop*, Cagliari, Italy, Sep. 2010, pp. 248–255.

[9] J. Lizarraga, P. Angeletti, N. Alagha, and M. Aloisio, "Multibeam satellites performance analysis in non-uniform traffic conditions," in *Proc. IEEE 14th Int. Vac. Electron. Conf. (IVEC)*, Paris, France, May 2013, pp. 7–8.

[10] F. Joly and M. Kluth, "Target 2 system architectural and design tradeoffs," DDS.DDD.00002.T.ASTR, ESA DDSO Study, Feb. 2005.

[11] X. Alberti, J. M. Cebrian, A. Del Bianco, Z. Katona, J. Lei, M. A. Vazquez-Castro, A. Zanus, L. Gilbert, and N. Alagha, "System capacity optimization in time and frequency for multibeam multi-media satellite systems," in *Proc. 5th Adv. Satell. Multimedia Syst. Conf., 11th Signal Process. Space Commun. Workshop*, Cagliari, Italy, Sep. 2010, pp. 226–233.

[12] J. Lei and M. A. Vazquez-Castro, "Multibeam satellite frequency/time duality study and capacity optimization," *J. Commun. Netw.*, vol. 13, no. 5, pp. 472–480, Oct. 2011.

[13] L. Wang, C. Zhang, D. Qu, and G. Zhang, "Resource allocation for beam-hopping user downlinks in multi-beam satellite system," in *Proc. 15th Int. Wireless Commun. Mobile Comput. Conf. (IWCMC)*, Tangier, Morocco, Jun. 2019, pp. 925–929.

[14] W. Liu, F. Tian, Z. Jiang, G. Li, and Q. Jiang, "Beam-hopping based resource allocation algorithm in LEO satellite network," in *Proc. Space Inf. Netw.*, Changchun, China, vol. 972, 2019, pp. 113–123.

[15] F. Tian, L. Huang, G. Liang, X. Jiang, S. Sun, and J. Ma, "An efficient resource allocation mechanism for beam-hopping based LEO satellite communication system," in *Proc. IEEE Int. Symp. Broadband Multimedia Syst. Broadcast. (BMSB)*, Jeju, South Korea, Jun. 2019, pp. 1–5.

[16] B. Koosha, H. J. Helgert, and R. Karimian, "A hybrid beam hopping design for non-uniform traffic in HTS networks," in *Proc. United States Nat. Committee URSI Nat. Radio Sci. Meeting (USNC-URSI NRSM)*, Boulder, CO, USA, Jan. 2019, pp. 1–2.

[17] R. Alegre-Godoy, N. Alagha, and M. A. Vazquez-Castro, "Offered capacity optimization mechanisms for multi-beam satellite systems," in *Proc. IEEE Int. Conf. Commun. (ICC)*, Ottawa, ON, Canada, Jun. 2012, pp. 3180–3184.

[18] J. P. Choi and V. W. S. Chan, "Optimum power and beam allocation based on traffic demands and channel conditions over satellite downlinks," *IEEE Trans. Wireless Commun.*, vol. 4, no. 6, pp. 2983–2992, Nov. 2005.

[19] M. J. Neely, E. Modiano, and C. E. Rohrs, "Power allocation and routing in multibeam satellites with time-varying channels," *IEEE/ACM Trans. Netw.*, vol. 11, no. 1, pp. 138–152, Feb. 2003.

[20] T. Zhang, L. Zhang, and D. Shi, "Resource allocation in beam hopping communication system," in *Proc. IEEE/AIAA 37th Digit. Avionics Syst. Conf. (DASC)*, London, U.K., Sep. 2018, pp. 1–5.
[21] H. Han, X. Zheng, Q. Huang, and Y. Lin, "QoS-equilibrium slot allocation for beam hopping in broadband satellite communication systems," *Wireless Netw.*, vol. 21, no. 8, pp. 2617–2630, Nov. 2015.
[22] L. Lei, E. Lagunas, Y. Yuan, M. G. Kibria, S. Chatzinotas, and B. Ottersten, "Beam illumination pattern design in satellite networks: Learning and optimization for efficient beam hopping," *IEEE Access*, vol. 8, pp. 136655–136667, 2020.
[23] L. Lei, E. Lagunas, Y. Yuan, M. G. Kibria, S. Chatzinotas, and B. Ottersten, "Deep learning for beam hopping in multibeam satellite systems," in *Proc. IEEE 91st Veh. Technol. Conf. (VTC-Spring)*, Antwerp, Belgium, May 2020, pp. 1–5.
[24] X. Hu, S. Liu, Y. Wang, L. Xu, Y. Zhang, C. Wang, and W. Wang, "Deep reinforcement learning-based beam hopping algorithm in multibeam satellite systems," *IET Commun.*, vol. 13, no. 16, pp. 2485–2491, Oct. 2019.
[25] C. Wang, D. Bian, S. Shi, J. Xu, and G. Zhang, "A novel cognitive satellite network with GEO and LEO broadband systems in the downlink case," *IEEE Access*, vol. 6, pp. 25987–26000, 2018.
[26] J. P. Choi and V. W. S. Chan, "Satellite multibeam allocation and congestion control with delay constraints," in *Proc. IEEE Int. Conf. Commun. (ICC)*, Paris, France, Jun. 2004, pp. 3309–3315.
[27] S. K. Sharma, S. Chatzinotas, and B. Ottersten, "Cognitive beamhopping for spectral coexistence of multibeam satellites," *Int. J. Satell. Commun. Netw.*, vol. 33, no. 1, pp. 69–91, Jan. 2015.
[28] C. Caruso, A. Colorni, and L. Aloi, "Dominant, an algorithm for the p-center problem," *Eur. J. Oper. Res.*, vol. 149, no. 1, pp. 53–64, Aug. 2003.
[29] Z. V. I. Drezner, "The p-centre problem-heuristic and optimal," *J. Oper. Res. Soc.*, vol. 35, no. 8, pp. 741–748, 1984.
[30] E. Welzl, "Smallest enclosing disks (balls and ellipsoids)," in *New Results and New Trends in Computer Science*, vol. 555, no. 3075. Graz, Austria: Springer, 1991, pp. 359–370.

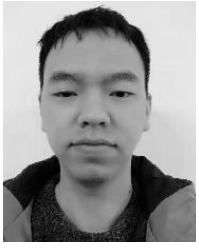

JINGYU TANG received the B.S. degree in telecommunications engineering from South China Normal University, China, in 2014, and the M.E. degree from the Army Engineering University of PLA, Nanjing, China, where he is currently pursuing the Ph.D. degree in communication engineering. His research interests include LEO satellite communications, dynamic resource management, and machine learning.

DONGMING BIAN received the Ph.D. degree from the PLA University of Science and Technology, Nanjing, China, in 2004. He is currently a Professor with the College of Communication Engineering, Army Engineering University of PLA, Nanjing. His research interests include wireless communications, satellite communications, and deep space communications.

GUANGXIA LI received the B.S. and M.S. degrees from the Institute of Communication Engineer, Nanjing, China, in 1983 and 1986, respectively. He is currently a Professor with the College of Communication Engineering, Army Engineering University of PLA, Nanjing. His current research interests include the design of communication systems, satellite communications, satellite navigation, communication anti-jamming, and satellite TT&C.

JING HU received the B.S. and M.S. degrees from the Nanjing University of Posts and Telecommunications, Nanjing, China, in 2003 and 2007, respectively. She is currently pursuing the Ph.D. degree with the College of Communications Engineering, Army Engineering University of PLA, Nanjing. Her current research interests include wireless communications, satellite communications, and communication anti-jamming.

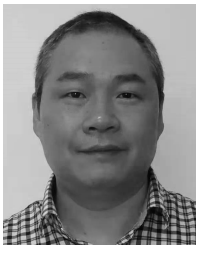

JIAN CHENG received the Ph.D. degree from the PLA University of Science and Technology, Nanjing, China, in 2008. He is currently a Professor with the College of Communication Engineering, Army Engineering University of PLA, Nanjing. His research interests include satellite communications, satellite TT&C, and satellite covert communication.